

available at www.sciencedirect.comjournal homepage: www.intl.elsevierhealth.com/journals/dema

Injectable and strong nano-apatite scaffolds for cell/growth factor delivery and bone regeneration^{☆,☆☆}

Hockin H.K. Xu^{a,*}, Michael D. Weir^a, Carl G. Simon^b

^a Department of Endodontics, Prosthodontics and Operative Dentistry, University of Maryland Dental School, Baltimore, MD 21201-1586, USA

^b National Institute of Standards and Technology, Gaithersburg, MD 20899-8546, USA

ARTICLE INFO

Article history:

Received 16 January 2008

Accepted 2 February 2008

Keywords:

Calcium phosphate cement

Nano-apatite

Macroporous scaffolds

Stress-bearing

Osteoblast cell delivery

Growth factor

Bone tissue engineering

ABSTRACT

Objectives. Seven million people suffer bone fractures each year in the U.S., and musculoskeletal conditions cost \$215 billion/year. The objectives of this study were to develop moldable/injectable, mechanically strong and *in situ*-hardening calcium phosphate cement (CPC) composite scaffolds for bone regeneration and delivery of osteogenic cells and growth factors.

Methods. Tetracalcium phosphate [TTCP: Ca₄(PO₄)₂O] and dicalcium phosphate (DCPA: CaHPO₄) were used to fabricate self-setting calcium phosphate cement. Strong and macroporous scaffolds were developed via absorbable fibers, biopolymer chitosan, and mannitol porogen. Following established protocols, MC3T3-E1 osteoblast-like cells (Riken, Hirosaka, Japan) were cultured on the specimens and inside the CPC composite paste carrier.

Results. The scaffold strength was more than doubled via reinforcement ($p < 0.05$). Relationships and predictive models were established between matrix properties, fibers, porosity, and overall composite properties. The cement injectability was increased from about 60% to nearly 100%. Cell attachment and proliferation on the new composite matched those of biocompatible controls. Cells were able to infiltrate into the macropores and anchor to the bone mineral-like nano-apatite crystals. For cell delivery, alginate hydrogel beads protected cells during cement mixing and setting, yielding cell viability measured via the Wst-1 assay that matched the control without CPC ($p > 0.1$). For growth factor delivery, CPC powder:liquid ratio and chitosan content provided the means to tailor the rate of protein release from CPC carrier.

Significance. New CPC scaffolds were developed that were strong, tough, macroporous and osteoconductive. They showed promise for injection in minimally invasive surgeries, and in delivering osteogenic cells and osteoinductive growth factors to promote bone regeneration. Potential applications include various dental, craniofacial, and orthopedic reconstructions.

© 2008 Academy of Dental Materials. Published by Elsevier Ltd. All rights reserved.

[☆] This article was presented as an invited talk at the Academy of Dental Materials Annual Meeting in Fort Lauderdale, FL, USA, October 2007.

^{☆☆} Certain commercial materials and equipment are identified in this paper to specify experimental procedures. In no instance does such identification imply recommendation by NIST. One standard deviation (S.D.) was used as the estimated standard uncertainty of the measurements unless otherwise specified in the Methods. These data should not be compared with those obtained in other laboratories under different conditions. Official contribution of the National Institute of Standards and Technology; not subject to copyright in the United States.

* Corresponding author at: Department of Endodontics, Prosthodontics and Operative Dentistry, University of Maryland Dental School, 650 West Baltimore Street, Baltimore, MD 21201, USA. Tel.: +1 410 706 7047; fax: +1 410 706 3028.

E-mail address: hxu@umaryland.edu (H.H.K. Xu).

0109-5641/\$ – see front matter © 2008 Academy of Dental Materials. Published by Elsevier Ltd. All rights reserved.

doi:10.1016/j.dental.2008.02.001

1. Introduction

Approximately 6.2 million fractures occurred in the U.S. each year from 1992 to 1994 [1,2]. In 1998, 7 million people suffered fractures [3]. In 1995, musculoskeletal conditions cost the U.S.\$ 215 billion [1,4]. These numbers are predicted to increase dramatically because of the increasing life expectancy [5,6]. Indeed, fractures in the elderly have recently seen a marked increase in frequency and severity [7]. Bioinert implants without bone-like calcium phosphate (CaP) mineral can form an undesirable fibrous capsule, while implants with bone-like mineral beneficially bond to native bone. This is because the biomimetic CaP mineral provides a preferred substrate for cell attachment and supports the proliferation and expression of osteoblast phenotype [8–10]. Hence, hydroxyapatite (HA) and other CaP bioceramics are important for hard tissue repair with their osteoconductivity and bone-bonding ability [11–18].

For sintered hydroxyapatite and other bioceramics to fit into a bone cavity, the surgeon needs to machine the graft to the desired shape or carve the surgical site around the implant. This leads to increases in bone loss, trauma and surgical time [5]. In contrast, calcium phosphate cements can be molded and set *in situ* to provide intimate adaptation to the contours of defect surfaces [19–23]. Calcium phosphate cement (CPC) is comprised of a mixture of tetracalcium phosphate [TTCP: $\text{Ca}_4(\text{PO}_4)_2\text{O}$] and dicalcium phosphate anhydrous (DCPA: CaHPO_4) [19]. The CPC powder can be mixed with an aqueous liquid to form a paste that can be sculpted during surgery to conform to the defects in hard tissues. The paste self-hardens to form resorbable hydroxyapatite [19]. Due to its excellent osteoconductivity and bone replacement capability, CPC is highly promising for a wide range of clinical applications [24–26]. As a result, CPC was approved in 1996 by the Food and Drug Administration for repairing craniofacial defects in humans, thus becoming the first CPC available for clinical use [25].

However, the brittleness and low strength limit the use of CPC to only non-load-bearing areas. Other deficiencies of CPC include its slow integration with adjacent bone due to the lack of macropores. The use of CPC was “limited to the reconstruction of non-stress-bearing bone” [24], and “none of the indications include significant stress-bearing applications” [25]. In periodontal repair, for example, tooth mobility resulted in the early fracture and eventual exfoliation of the brittle CPC implants [27]. Other potential dental and craniofacial uses of an improved CPC include mandibular and maxillary ridge augmentation, since CPC could be molded to the desired shape and set to form a scaffold for bone ingrowth. However, these implants would be subject to early loading by provisional dentures and need to be resistant to flexure. Major reconstructions of the maxilla or mandible after trauma or tumor resection would require a moldable implant with improved fracture resistance and rapid osteoconduction, as would the support of metal dental implants or augmentation of deficient implant sites. All these dental and craniofacial applications and many other orthopedic repairs would be better served with a highly biocompatible material, like an improved CPC, with better

fracture resistance and more rapid bone regeneration via macropores and the delivery of osteogenic cells and growth factors. This article describes recent experiments on tetracalcium phosphate–dicalcium phosphate cement scaffolds, focusing on injectable nano-apatite scaffolds and carriers for osteogenic cell and growth factor delivery for bone tissue engineering.

2. CPC composite scaffolds with tailored macropore formation rates

Macropores have been built into biomaterials to facilitate bony ingrowth and implant fixation. One advantage of a macroporous CPC is that it can form macroporous hydroxyapatite implants *in situ* without sintering and machining. However, macropores degraded the CPC strength by an order of magnitude. After macroporous materials are implanted, the strength of the implants significantly increases once new bone starts to grow into the macropores [28]. Therefore, it is in the early stage of implantation when the macroporous implant is in the most need of strength and toughness.

In a recent study [29], large-diameter absorbable fibers were incorporated in CPC to provide initial strengthening and then dissolved and created macropores for the first time. The short-term strength of CPC was thus substantially increased, and the subsequent fiber degradation created macropores in CPC for cell infiltration [29].

An approach to combine absorbable fibers and fast-dissolving porogens was used to develop strong scaffolds with controlled strength histories and tailored macropore formation rates. The rationale for this design was that CPC containing fast-dissolving mannitol and slow-dissolving fibers would have two stages of macropore formation *in vivo*: Mannitol would dissolve quickly upon contact with the physiological solution to form macropores to start tissue ingrowth, while the fibers would provide the needed early-strength to the graft. After significant new bone ingrowth into the macropores thus increasing the CPC strength, the fibers would then dissolve and create the second group of macropores for further tissue ingrowth. The fiber degradation rate can be controlled to match the new bone formation rate for specific applications.

TTCP was synthesized from a solid-state reaction between CaHPO_4 and CaCO_3 (Baker, NJ) and then ground to obtain a median particle size of 17 μm . The DCPA powder (Baker Chemical) was ground to obtain a median particle size of 1 μm . The TTCP and DCPA powders were mixed in a blender (Dynamics Corporation of America, New Hartford, CT) to form the CPC powder with a TTCP:DCPA molar ratio of 1.

Water-soluble mannitol crystals were used to produce macropores in CPC [30,31]. Mannitol was selected because it has the appropriate solubility, is non-toxic, and is physiologically compatible. Mannitol ($\text{CH}_2\text{OH}[\text{CHOH}]_4\text{CH}_2\text{OH}$, Sigma, St. Louis, MO) was recrystallized in an ethanol/water solution at 50/50 (v/v), filtered, ground, and sieved through openings of 500 μm (top sieve) and 300 μm (bottom sieve). The mannitol crystals thus obtained were mixed with CPC powder at a mannitol/(mannitol + CPC powder) mass fraction of 50% to form the CPC–mannitol powder.

Chitosan and its derivatives are natural biopolymers found in arthropod exoskeletons. They are biocompatible, biodegradable and hydrophilic. The cement liquid consisted of chitosan lactate (Technical grade, VANSON, Redmond, WA; referred to as chitosan) mixed with water to form the cement liquid. Although chitosan is not bioactive, the bioactivity can be provided by CPC in a CPC–chitosan composite. The purpose of incorporating chitosan into CPC was to strengthen and toughen the CPC.

An absorbable suture fiber (Vicryl™, Ethicon, Somerville, NJ) was cut to 8-mm long filaments as in a previous study [29]. This suture consisted of fibers braided into a bundle with a diameter of approximately 322 μm, suitable for producing macropores after fiber dissolution as described in a previous study [29]. The CPC–mannitol powder was mixed with the chitosan liquid, and then randomly mixed with the fibers. A fiber volume fraction of 30% was used in CPC [32]. The mixed paste was placed in rectangular molds of 3 mm × 4 mm × 25 mm. The specimen in each mold was covered with two mechanically clamped glass slides and set in a humidifier with 100% relative humidity for 4 h at 37 °C. The hardened specimens were demolded and immersed in a physiological solution at 37 °C to dissolve the porogens and form macropores. Examples of the two groups of macropores in a CPC scaffold are shown in Fig. 1.

3. Relationship between scaffold matrix, fiber, and composite properties

While the use of absorbable fibers and porogen successfully produced strong and macroporous CPC, the microstructural relationships need to be determined. A group of CPC specimens without fibers were fabricated; the mechanical properties of the CPC matrix were measured at different times after powder–liquid mixing to obtain a wide range of matrix properties [33,34]. A second group of specimens were made with the reinforcement of absorbable fibers. The strength of the fiber composite were measured and plotted as a function of matrix strength in Fig. 2A.

In a previous study on fiber reinforcement of CPC, an empirical equation was obtained that relates the CPC–fiber composite strength, S_C , to the fiber strength, S_F [35]:

$$S_C = S_m + \alpha S_F \quad (1)$$

where S_m is the strength of the matrix, and α is a coefficient. In that study, the matrix was held constant while S_F was varied by using different types of fibers [35]. In the present study, S_F was kept constant, while the CPC matrix was varied by changing the incubation time. The coefficient α in Eq. (1) should be proportional to S_m because when the CPC paste did not set, $S_m = 0$ and $S_C = 0$, thus requiring that $\alpha = 0$. This is because there was no matrix to support the fibers. Hence we assume $\alpha = \beta S_m$ to satisfy the condition that in Eq. (1), when $S_m = 0$, so should S_C , even when S_F is not zero. Therefore, $S_C = S_m + \beta S_m S_F = S_m (1 + \beta S_F)$, and finally

$$S_C = \gamma S_m \quad (2)$$

where $\gamma = 1 + \beta S_F$. Fig. 2A plots the measured composite strength S_C vs. the corresponding CPC matrix strength S_m . The straight line in Fig. 2A is a linear best-fit through the origin with a correlation coefficient $R^2 = 0.87$, yielding

$$S_C = 2.16 S_m \quad (3)$$

This suggests that (i) when the fiber type, fiber length and fiber volume fraction were kept constant, the composite strength increased linearly when the matrix strength was increased and (ii) the CPC composite strength was, in general, 2.16 times higher than the strength of CPC without fibers, when the suture fibers at 25% volume fraction and 8-mm length were randomly mixed into the CPC paste.

Another important parameter is the strength of the fibers inside the composite. Previous studies observed that when the fiber strength was degraded, the composite's behavior changed from a toughened mode to a brittle mode of failure [36,37]. Few experiments have yielded a quantitative relationship between fiber strength and the strength of calcium phosphate composites. Such a relationship would be important because it would not only provide guidance in material design and fabrication, but also give information on predicting the performance based on constituent properties.

To investigate this relationship, CPC–fiber specimens were fabricated and immersed in a physiological solution at 37 °C for 1–119 days. To measure the strength of the suture fiber, filaments with a length of 25 mm were also immersed in the same physiological solution. To determine the tensile strength of the fiber, the fiber diameter was measured. The tensile strength of the fiber was measured by fracturing in uniaxial tension with a gauge length of 8 mm and a crosshead speed of 1 mm/min on a computer-controlled Universal Testing Machine (model 5500R, Instron, MA). The break load divided by the cross-section area of the fiber yielded the fiber strength.

The CPC composite strength S_C , and suture fiber strength S_F , were fitted to the measured data by linear regression, yielding the following equation:

$$S_C = 14.1 + 0.047 S_F \quad (4)$$

Fig. 2B plots S_C vs. the corresponding S_F with correlation coefficient $R^2 = 0.85$. This equation shows that a key to increasing the CPC composite strength is to develop stronger fibers. In addition, the fiber needs to be tailored so that it maintains a high strength for a desired period of time to match specific rate of new bone formation [38].

Relationships were also determined between scaffold porosity and strength and fracture toughness. Chitosan and mannitol were incorporated into CPC: chitosan to make the material stronger and anti-washout; and mannitol to create macropores in CPC. Flexural strength, elastic modulus, and fracture toughness were measured. After mannitol dissolution in a physiological solution, macropores were formed in CPC in the shapes of the original entrapped mannitol crystals, with diameters of 50–200 μm for cell infiltration and bone ingrowth. The resulting porosity in CPC ranged from 34% to 83% volume fraction [39].

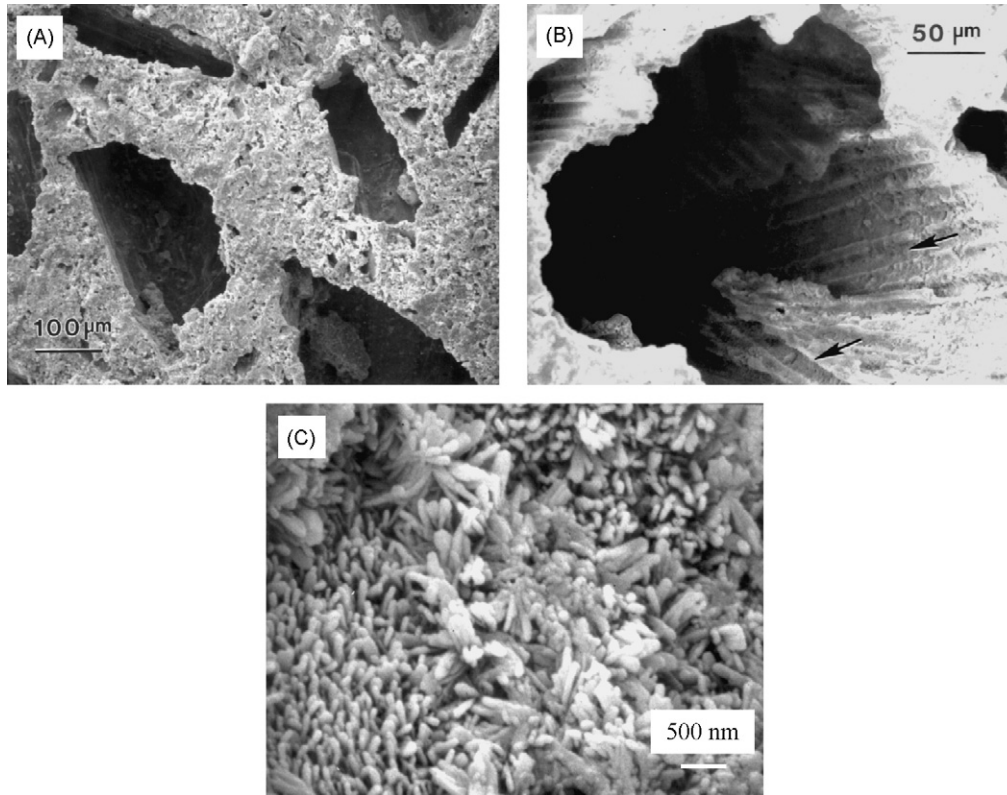


Fig. 1 – (A) The first group of macropores was formed in CPC via the dissolution of mannitol during 1-day of immersion, while fibers in CPC provide the needed early strength. (B) The second group of macropores was formed in CPC by the dissolution of fibers after 17 weeks of immersion. The rationale was that after being implanted for several weeks in vivo, new bone would have grown into the first group of macropores to increase the CPC strength. (C) Nano-hydroxyapatite crystals that make up the CPC matrix.

Previous studies have modeled porous ceramics as an elastic-brittle foam and yielded the following relationship [13]:

$$S = \alpha d^x \quad (5)$$

where S is flexural strength, d is specimen density, and α and x are constants. The density of the scaffold $d = d_0(1 - P)$, where d_0 is the density of the fully dense material, and P is the pore volume fraction of the scaffold. Inserting this into Eq. (5) yields

$$S = S_0(1 - P)^x \quad (6)$$

Eq. (6) shows that when porosity $P = 1$, $S = 0$. When $P = 0$ (fully dense), $S = S_0$, which is the strength for fully dense specimens. Assuming that the same relationship also holds for fracture toughness, K_{IC} :

$$K_{IC} = K_{IC0}(1 - P)^z \quad (7)$$

where z is a constant and K_{IC0} is toughness for fully dense specimens.

By fitting Eqs. (6) and (7) to the measured properties, the best fits were obtained and are shown in Fig. 2C and D. The solid lines in Fig. 2C and D are regression power-law fits to the measured data, with $R^2 = 0.98$. The regression coefficients

resulted in the following relationships:

$$S = 94.9(1 - P)^{3.3} \text{ MPa} \quad (8)$$

$$K_{IC} = 0.86(1 - P)^{2.1} \text{ MPa m}^{1/2} \quad (9)$$

The fitting yielded $S_0 = 94.9 \text{ MPa}$ for flexural strength of fully dense specimens, which is within the reported bending strength range of 38–250 MPa for dense hydroxyapatite [12]. For fracture toughness, the fitting yielded $K_{IC0} = 0.86 \text{ MPa m}^{1/2}$ for fully dense specimens, consistent with the reported range of 0.8–1.2 $\text{MPa m}^{1/2}$ for dense hydroxyapatite [12]. While the general relationships in Eqs. (6) and (7) may be applicable to other scaffold systems, the actual coefficients are expected to be material-specific and will need to be individually determined to establish models such as Eqs. (8) and (9).

4. Injectability of macroporous CPC scaffold

Besides strength and toughness, the injectability of CPC is also of critical importance for use in minimally invasive techniques such as *in situ* fracture fixation, and percutaneous vertebroplasty to fill and strengthen osteoporotic bone lesions at risk for fracture. The advantages of developing an injectable CPC

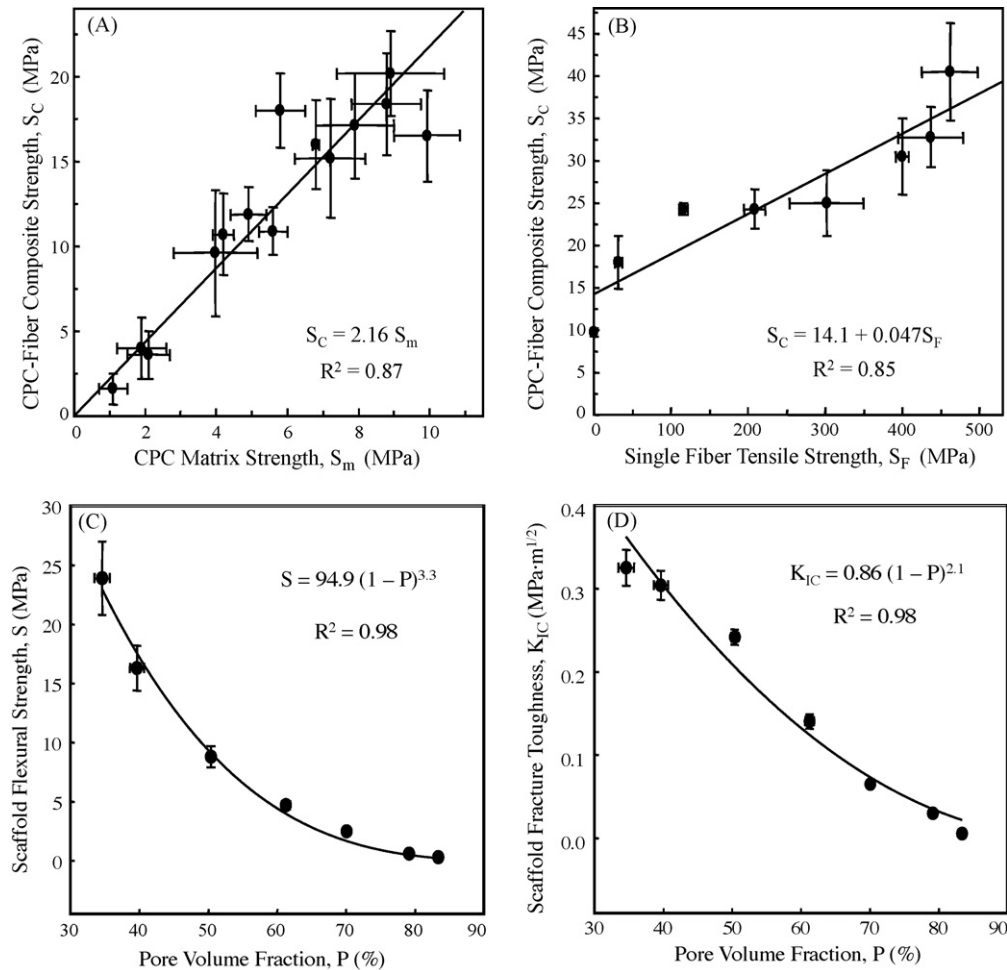


Fig. 2 – Relationships between scaffold matrix property, fiber property, and composite property. (A) CPC composite–CPC matrix relationship. (B) CPC fiber composite–individual fiber relationship. (C) CPC scaffold strength–porosity volume fraction relationship. (D) Fracture toughness–porosity relationship. Each value is mean \pm S.D.; $n = 6$. Each curve is the best fit to the experimental data as described in the text.

include: (i) Shortening the surgical operation time; (ii) minimizing the damaging effects of large muscle retraction; (iii) reducing postoperative pain and scar size; (iv) achieving rapid recovery; (v) reducing cost. However, traditional CPC is poorly injectable. In Fig. 3(A), the injectability of two CPC pastes was measured [34]. The injectability, I , was defined as the mass of CPC paste that was extruded from the syringe under a maximum load of 100 N, divided by the original mass of paste in the syringe. CPC_A denotes the use of TTCP and DCPA powders, while CPC_D refers to the use of TTCP and DCPD (dicalcium phosphate dehydrate, CaHPO₄·2H₂O) powders [34]. Note in Fig. 3A that without HPMC, only about 60% of the CPC paste was extruded, confirming observations of surgeons that traditional CPC has a poor injectability. However, the injectability was dramatically improved when a gelling agent, hydroxypropyl methylcellulose (HPMC), was added [34]. In Fig. 3B, using 1% HPMC, the paste was fully injectable with an injection force of less than 20 N, even when the paste contained mannitol porogen of up to 40%. The purpose of porogen was to subsequently create macropores after the porogen particles were dissolved in the physiological solution. Therefore,

the first fully injectable, macroporous CPC scaffold was thus developed.

5. Cell infiltration into scaffold

Because cell culture toxicity assays are the international standard for biocompatibility screening [40], *in vitro* cell culture was performed to evaluate the biocompatibility of the new CPC scaffolds. MC3T3-E1 osteoblast-like cells (Riken, Hirosaka, Japan) were cultured following established protocols [40–42]. Cells were cultured in flasks at 37 °C and 100% humidity with 5% CO₂ (volume fraction) in α modified Eagle's minimum essential medium (Biowhittaker, Walkersville, MD). The medium was supplemented with 10% volume fraction of fetal bovine serum (Gibco, Rockville, MD) and kanamycin sulfate (Sigma, St. Louis, MO). Cultures of 90% confluent cells were trypsinized, washed and suspended in fresh media. Traditional CPC control and new, mechanically stronger CPC scaffold composites were tested. Fifty thousand cells diluted into 2 mL of media were added to each well containing a speci-

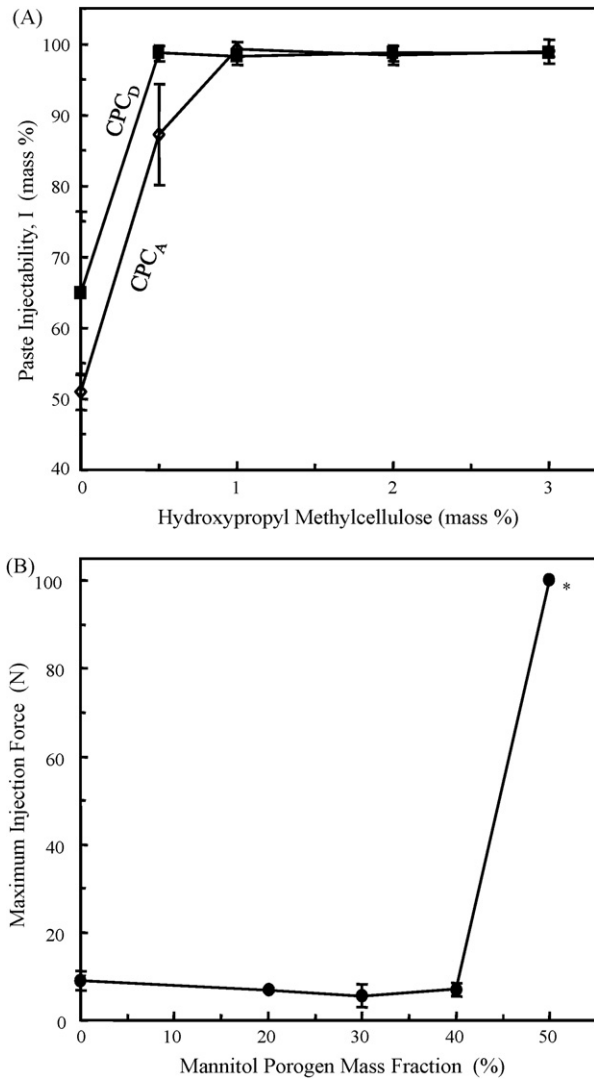


Fig. 3 – (A) The injectability for two different CPC pastes. Note the poor injectability without HPMC. Adding a small amount of HPMC dramatically improved the injectability. (B) The force required to inject the CPC paste containing mannitol porogen particles, which were later dissolved in a physiological solution to create macropores in the injectable CPC. The paste contained 1% HPMC. The CPC was fully injectable having up to 40% mannitol. The * in (B) indicates that the maximum force of 100 N was reached.

men or to an empty well of tissue culture polystyrene (TCPS, as a biocompatible control), and incubated for 1 or 14 days (2 mL of fresh media every 2 days) [42,43].

After 1 or 14 days incubations of the cells on the CPC–chitosan, CPC control or TCPS control, the media was removed and the cells were washed two times in 2 mL of Tyrode's Hepes buffer (140 mmol/L NaCl, 0.34 mmol/L Na₂HPO₄, 2.9 mmol/L KCl, 10 mmol/L Hepes, 12 mmol/L NaHCO₃, 5 mmol/L glucose, pH 7.4). Cells were stained and viewed by epifluorescence microscopy (Eclipse TE300, Nikon, Melville, NY). The results are shown in Fig. 4. Staining of cells was done for 5 min with 2 mL of Tyrode's Hepes buffer containing calcein-AM and ethidium homodimer-1 (both from

Molecular Probes, Eugene, OR). Calcein-AM is a nonfluorescent, cell-permeant fluorescein derivative, which is converted by cellular enzymes into cell-impermeant and highly fluorescent calcein. Calcein accumulates inside live cells having intact membranes causing them to fluoresce green. Ethidium-homodimer-1 enters dead cells with damaged membranes and undergoes a 40-fold enhancement of fluorescence upon binding to their DNA causing the nuclei of dead cells to fluoresce red. Double-staining allows simultaneous examination of both live and dead cells anchored on the materials.

Selected specimens were examined via a scanning electron microscope (SEM, JEOL 5300, Peabody, MA). Cells cultured for 1 day while anchored onto the specimens were rinsed with saline, fixed with 1% volume fraction of glutaraldehyde, subjected to graded alcohol dehydrations, rinsed with hexamethyldisilazane, and sputter coated with gold. The results are shown in Fig. 5.

6. Cell delivery

The introduction of stem cells into the clinical setting opens new horizons. Embryonic and fetal stem cells are pluripotent, able to become over 200 types of cells in the body. Adult mesenchymal (or stromal) stem cells derived from the bone marrow are multipotent, able to differentiate into neural tissue, cartilage, bone, and fat. Human mesenchymal stem cells (hMSC) are emerging as an important tool to engineer bone tissues. hMSCs can be harvested from the patient's bone marrow, expanded in culture, and combined with a scaffold carrier to deliver the cells to bone defects. A high seeding efficiency can minimize growth time and facilitate healing. However, seeding cells uniformly deep into the interior of a pre-formed scaffold is a serious challenge. *In vitro* tissue-engineering constructs thicker than 1 mm often result in a shell of viable cells and new extracellular matrix surrounding a necrotic core. CPC has a significant advantage in this regard, because it comes in the form of a paste, not a pre-formed scaffold. Therefore, it has the potential to have the cells incorporated uniformly throughout the entire volume of the paste. The cell-seeded paste can then be placed *in vivo* and harden *in situ* to form a macroporous, biomimetic nano-apatite scaffold.

In preliminary experiments, MC3T3-E1 cells were seeded onto the CPC paste, incubated for 24 h and double-stained to be green for live cells and red for dead cells. The results in Fig. 6 show that the cement setting reaction was harmful to the cells. However, once it was set, CPC was biocompatible and supported cell attachment and proliferation. Therefore, short-term protection was needed for the cells during cement mixing and setting.

Alginate was used as an encapsulating gel to protect the cells. Alginate is biocompatible and can form a crosslinked gel under mild conditions [44]. A 1.2% (mass fraction) sodium alginate solution was prepared by dissolving 0.3 g alginate (UP LVG, 64% guluronic acid, MW = 75,000–220,000 g/mol, ProNova Biomedical, Oslo, Norway) in 25 mL of saline (155 mmol/L NaCl). Cells were encapsulated in alginate at a density of 100,000 cells/mL of alginate solution for the live/dead staining experiment, and 500,000 cells/mL for the Wst-1 experiment. This resulted in the number of encapsulated cells being

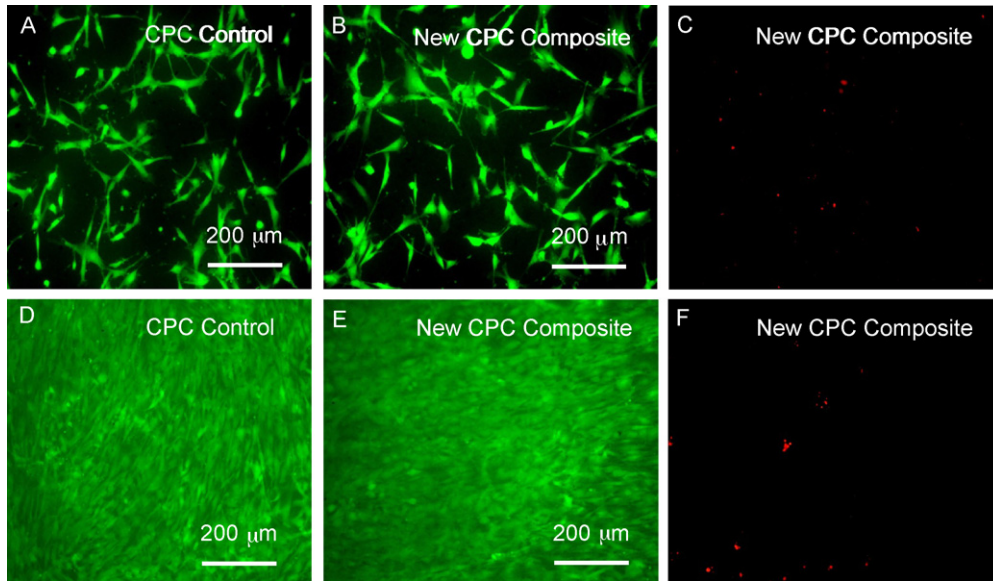


Fig. 4 – (A–C) After 1-day culture, live cells (stained green) appeared to have adhered and attained a normal polygonal morphology on the specimen. Dead cells (stained red) in (C) were very few on both materials. **(D–F)** After 14 days of culture, live cells had formed a confluent monolayer on all specimens. The cell density was much greater than the 1-day density, indicating that the cells had greatly proliferated. These results suggest that cell proliferation was similar, demonstrating that the new CPC composite was as non-cytotoxic as the FDA-approved CPC control and the TCPS control.

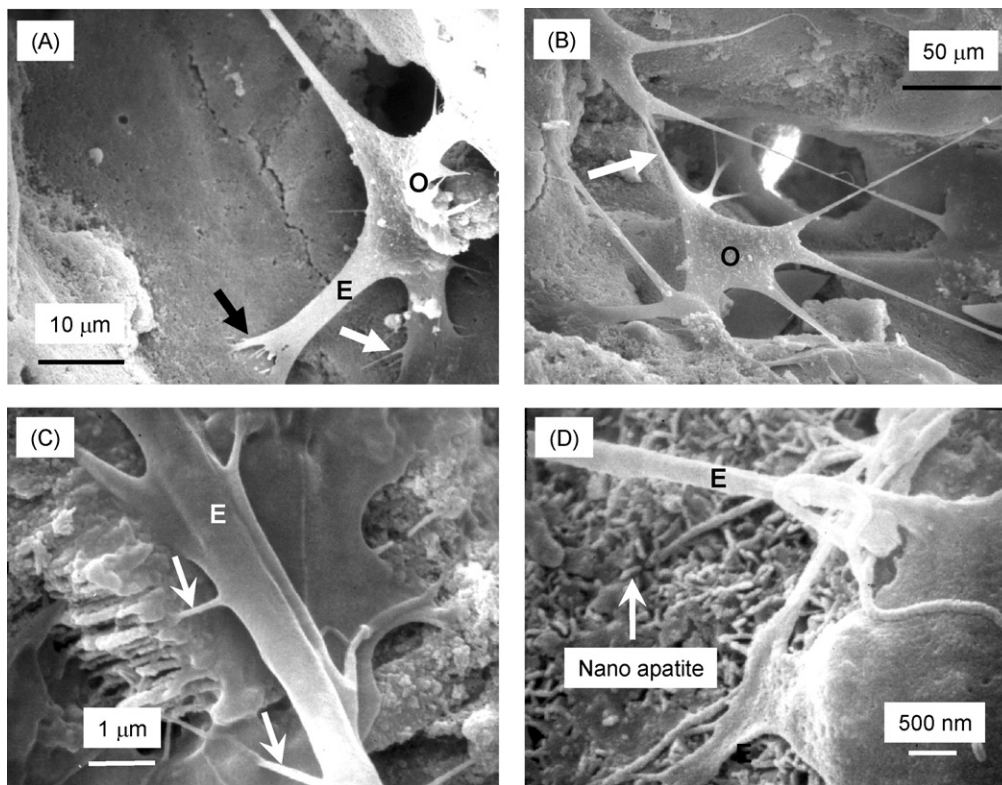


Fig. 5 – SEM micrographs showing cell infiltration into the macropores of CPC scaffolds. (A) The pore was large enough for the osteoblast cell “O”, and the cell had developed long cytoplasmic extensions “E” anchoring to the pore bottom. **(B)** Two cells had established cell–cell junction (arrow) in the pore. **(C)** High magnification shows secondary extensions sprouting from the primary extension “E”. **(D)** Cell extensions anchored to the nano-apatite crystals that make up the CPC matrix.

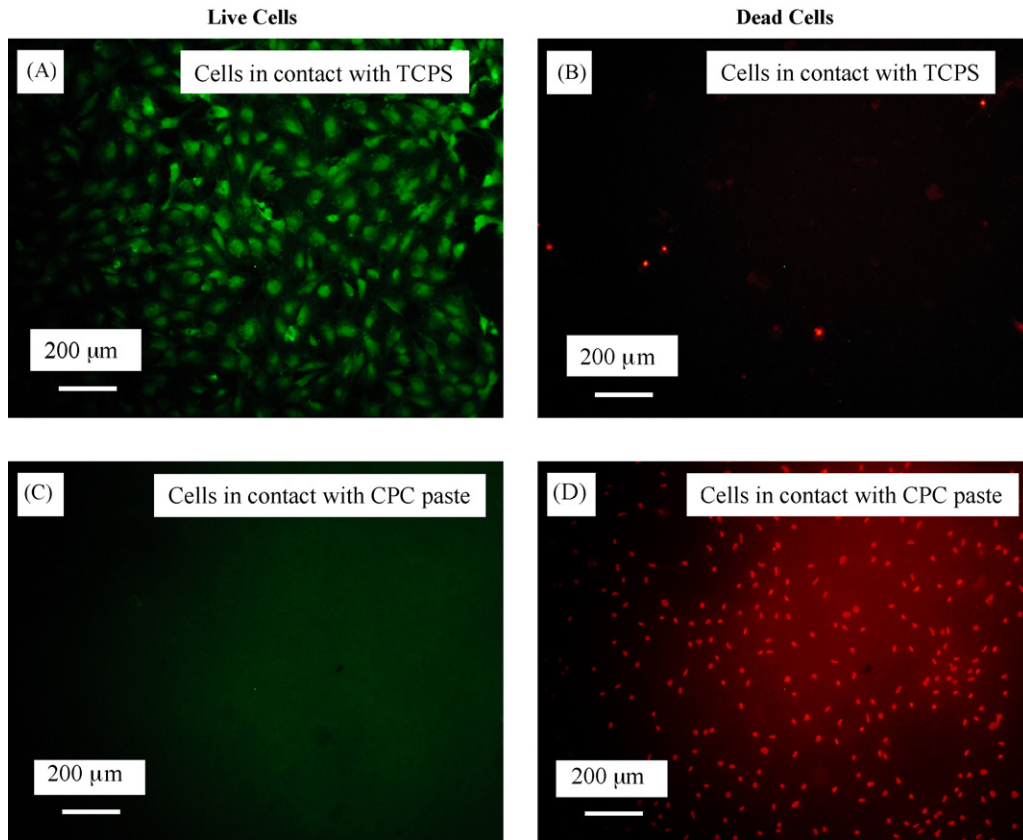


Fig. 6 – For cell delivery via the CPC paste carrier, the cement paste setting reaction was harmful to the cells, as shown in (C) and (D). However, once the cement was set, it was biocompatible and supported cell attachment and proliferation. Therefore, cell protection was needed during cement mixing and setting.

558 cells/bead and 2790 cells/bead, respectively. Bead formation was accomplished by extruding alginate/cell droplets through a sterile syringe fitted with a 25-gauge needle into wells containing 7 mL of 100 mmol/L calcium chloride solution. The alginate droplets crosslinked and formed beads in the calcium chloride solution.

The results in Fig. 7 show that the alginate beads successfully protected the cells from the setting of a CPC paste, a CPC–chitosan paste, and a composite paste of CPC–chitosan–mesh. The alginate hydrogel beads served three functions: (1) as a vehicle to deliver cells and nutrients into CPC–chitosan and CPC–chitosan–mesh composites; (2) to protect the cells from environmental changes during cement setting; and (3) to generate a porous structure in CPC via subsequent degradation of the hydrogel beads [45].

7. Protein/growth factor delivery

Incorporation of growth factors into bone graft is highly beneficial in tissue engineering [46–49]. Protein A, fluorescently labeled with fluorescein isothiocyanate (FITC), was used as a model compound for growth factor release from CPC–chitosan composite. Protein A (Sigma, St. Louis, MO) is a cell surface receptor with a molecular weight of 42 kDa ($Da = g/mol$ and stands for Daltons, and is a measure of molecular mass for

proteins and biological molecules). It was selected because it was similar in size and structure to bone morphogenetic protein-2 and transforming growth factor- β , and because previous studies indicated that protein A was a suitable model protein for release measurements [50]. The relative molecular mass of protein A was close to the 36 kDa of bone morphogenetic protein-2 (BMP-2), and the 25 kDa of transforming growth factor- β (TGF- β), while protein A was much less expensive [51,52]. In the present study, as-received FITC-labeled protein A was obtained from Sigma. Aliquots were made in phosphate-buffered saline (pH of 7.2) at a concentration of 5 mg/mL, and were kept frozen at $-80^{\circ}C$ until needed [53].

Protein A-FITC was added to the CPC liquid at a concentration of 100 ng/mL. To measure protein release from the set CPC scaffold, the fluorescence emission intensity of FITC-labeled protein A was measured using a microplate reader (Wallac 1420 Victor², PerkinElmer Life Science, Gaithersburg, MD) [53]. Each specimen of 3 mm \times 4 mm \times 12 mm was placed into a 15 mL centrifuge tube, 10 mL of PBS (pH 7.2) was added. Centrifuge tubes were placed in a 37 $^{\circ}C$ incubator. The protein release profiles thus measured are plotted in Fig. 8.

When only a buffer was used as a carrier for bone morphogenic protein (BMP), results indicated that there was a reduced number of responsive stem cells and insufficient retention of BMP at the repair site to promote bone regeneration [54]. Alternately, slowly releasing BMPs from an

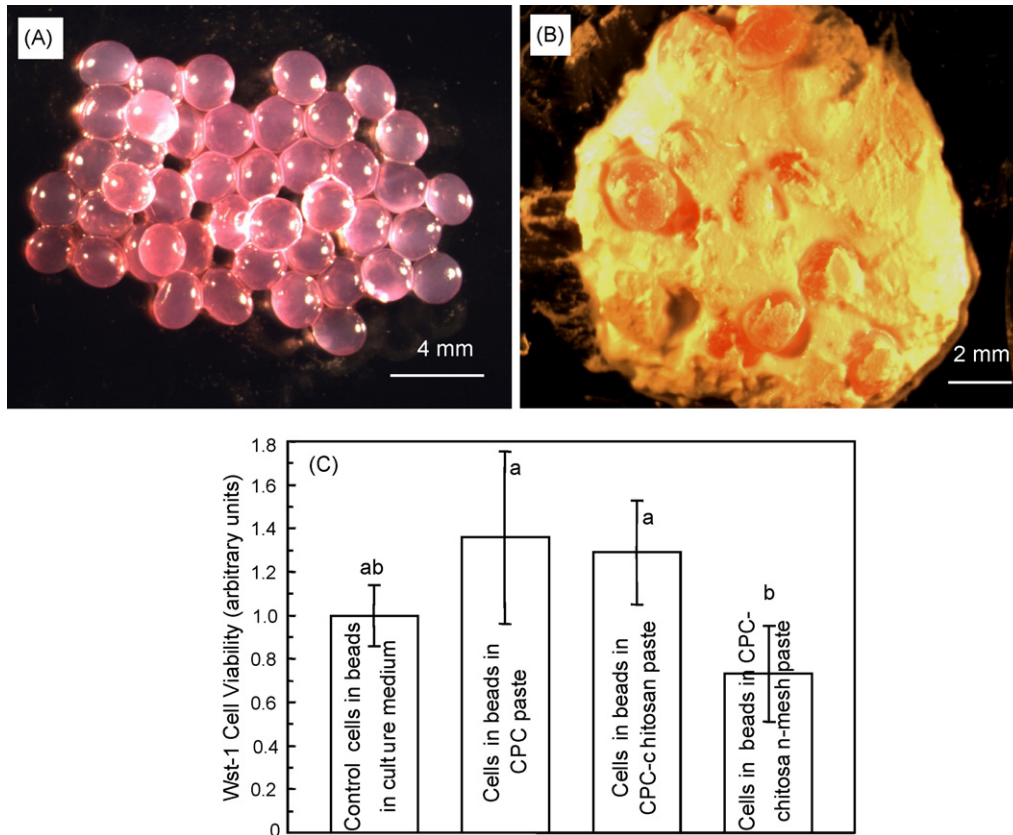


Fig. 7 – Cell delivery via CPC composite-hydrogel construct. (A) Cell-seeded alginate hydrogel beads. Cells were encapsulated into alginate beads which were then mixed into three pastes: conventional CPC, CPC–chitosan, and CPC–chitosan–mesh. **(B)** CPC paste mixed with the cell-seeded hydrogel beads. After 1-day culture inside the setting cements, there were numerous live cells and very few dead cells, indicating that the alginate beads adequately protected the cells. The cell viability (mean \pm S.D.; $n = 5$) after 14 days was measured using the Wst-1 assay. The absorbance at 450 nm was (1.36 ± 0.41) for the conventional CPC and (1.29 ± 0.24) for CPC–chitosan composite, similar to the (1.00 ± 0.14) for the control with the beads in the culture medium without any CPC ($p > 0.1$).

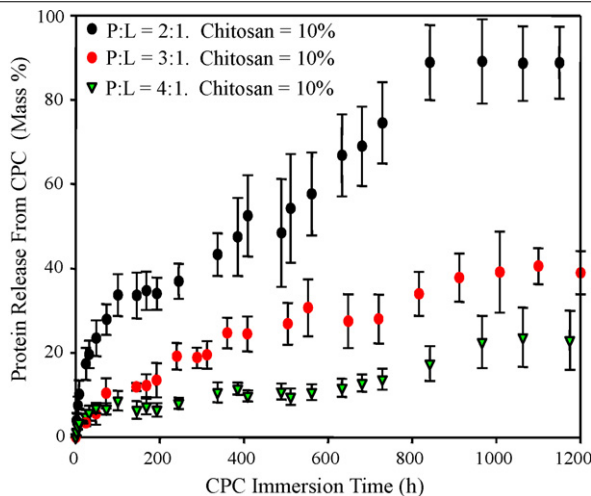


Fig. 8 – Protein release from CPC carrier for a growth factor release study. The cement powder:liquid ratio had a significant effect on protein release ($p < 0.05$). Powder:liquid ratio and chitosan content are shown to be key microstructural parameters that can be tailored to control the protein release profile from CPC to be application-specific [51].

appropriate carrier could provide a physiological concentration of BMPs in the implant area and allow cells to be attracted by chemotaxis [55]. Along with the retention of BMPs at the repair site, BMPs mixed with CPC would be beneficial due to the fact that their bioactivity could be maintained [56]. In order for a particular bone graft therapy to be clinically relevant, an appropriate carrier must be designed that will maintain therapeutic levels of diffusible growth factors/proteins at the repair site. Fig. 8 shows that for the CPC with 10% chitosan at a powder:liquid ratio of 3:1, the released protein mass fraction was about 0.4 (or 40%). Hence more than half of the protein was still retained in the CPC after 1200 h of immersion. Therefore, a sustained protein release from such a reservoir is expected to occur as the hydroxyapatite matrix is gradually resorbed while new bone is being formed *in vivo*. Further animal studies are needed to investigate bone regeneration via CPC/growth factor constructs.

8. Summary

Moldable/injectable, mechanically strong and *in situ*-hardening CPC composite scaffolds were formulated via

absorbable fibers, biopolymer chitosan, and mannitol porogen. The relationships between matrix, fiber, porosity and composite properties were established. The injectability was substantially improved. Macropores suitable for cell infiltration were created in the nano-apatite matrix. The new composites were non-cytotoxic and supported the adhesion, spreading, proliferation and viability of osteoblast-like cells. Osteoblast cells were able to infiltrate into the macropores, establish cell–cell junctions, and anchor to the nano-apatite walls of the pores. Furthermore, cell–CPC–chitosan–mesh constructs were formulated for cell delivery. Alginate hydrogel beads adequately protected the cells from the cement setting reaction. In addition, protein release from CPC could be regulated to be application-specific by altering the powder to liquid ratio and chitosan content, thereby altering the scaffold porosity. The relatively high-strength and osteoconductive CPC composites may be an effective delivery vehicle for osteoinductive growth factors, antibiotics and other molecules necessary to promote bone regeneration. Potential dental and craniofacial uses of an improved CPC include mandibular and maxillary ridge augmentation, since CPC could be molded to the desired shape and set to form a scaffold for bone ingrowth. However, these implants would be subject to early loading by provisional dentures and need to be resistant to flexure. Major reconstructions of the maxilla or mandible after trauma or tumor resection would require a moldable implant with improved fracture resistance and rapid osteoconduction, as would the support of metal dental implants or augmentation of deficient implant sites. Other potential uses include minimally invasive surgeries such as *in situ* fracture fixation and percutaneous vertebroplasty to fill and strengthen osteoporotic bone lesions at risk for fracture. Furthermore, the methods of developing moldable/injectable macroporous scaffolds, reinforcement, processing–structure–property relationships, and the delivery of growth factors and cells, may have wide applicability to other tissue engineering systems.

Acknowledgments

We thank S. Takagi, L.C. Chow, E.F. Burguera, Y. Zhang, and A.A. Giuseppetti for discussions and help. This study was supported by USPHS NIH grant R01 DE14190 (to Xu).

REFERENCES

- [1] Praemer A, Furner S, Rice DP. Musculoskeletal conditions in the United States. Rosemont: Amer Acad Orthop Surg; 1999 [chapter 1].
- [2] Franceshi RT. Biological approaches to bone regeneration by gene therapy. *Crit Rev Oral Biol Med* 2005;84:1093–103.
- [3] Medical Data International. RP-651147—Orthopedic and musculoskeletal markets: Biotechnology and Tissue Engineering. 2000; p. 28–31.
- [4] Ambrosio AMA, Sahota JS, Khan Y, Laurencin CT. A novel amorphous calcium phosphate polymer ceramic for bone repair. I. Synthesis and characterization. *J Biomed Mater Res* 2001;58B:295–301.
- [5] Laurencin CT, Ambrosio AMA, Borden MD, Cooper JA. Tissue engineering: orthopedic applications. *Annu Rev Biomed Eng* 1999;1:19–46.
- [6] Hench LL, Polak JM. Third-generation biomedical materials. *Science* 2002;295:1014–7.
- [7] An YH. Internal fixation in osteoporotic bone. New York, NY: Thieme Medical, 2002, Foreword.
- [8] Murphy WL, Hsiong S, Richardson TP, Simmons GA, Mooney DJ. Effects of a bone-like mineral film on phenotype of adult human mesenchymal stem cells *in vitro*. *Biomaterials* 2005;26:303–10.
- [9] Livingston T, Ducheyne P, Garino J. *In vivo* evaluation of a bioactive scaffold for bone tissue engineering. *J Biomed Mater Res* 2002;62:1–13.
- [10] Ehara A, Ogata K, Imazato S, Ebisu S, Nakano T, Umakoshi Y. Effects of alpha-TCP and TetCP on MC3T3-E1 proliferation, differentiation and mineralization. *Biomaterials* 2003;24:831–6.
- [11] LeGeros RZ. Biodegradation and bioresorption of calcium phosphate ceramics. *Clin Mater* 1993;14:65–88.
- [12] Suchanek W, Yoshimura M. Processing and properties of hydroxyapatite-based biomaterials for use as hard tissue replacement implants. *J Mater Res* 1998;13:94–117.
- [13] Hing KA, Best SM, Bonfield W. Characterization of porous hydroxyapatite. *J Mater Sci: Mater Med* 1999;10:135–45.
- [14] Ducheyne P, Qiu Q. Bioactive ceramics: the effect of surface reactivity on bone formation and bone cell function. *Biomaterials* 1999;20:2287–303.
- [15] Pilliar RM, Filiaggi MJ, Wells JD, Grynypas MD, Kandel RA. Porous calcium polyphosphate scaffolds for bone substitute applications – *in vitro* characterization. *Biomaterials* 2001;22:963–72.
- [16] Chu TMG, Orton DG, Hollister SJ, Feinberg SE, Halloran JW. Mechanical and *in vivo* performance of hydroxyapatite implants with controlled architectures. *Biomaterials* 2002;23:1283–93.
- [17] Foppiano S, Marshall SJ, Marshall GW, Saiz E, Tomsia AP. The influence of novel bioactive glasses on *in vitro* osteoblast behavior. *J Biomed Mater Res A* 2004;71:242–9.
- [18] Russias J, Saiz E, Deville S, Gryn K, Liu G, Nalla RK, et al. Fabrication and *in vitro* characterization of three-dimensional organic/inorganic scaffolds by robocasting. *J Biomed Mater Res A* 2007;83:434–45.
- [19] Brown WE, Chow LC. A new calcium phosphate water setting cement. In: Brown PW, editor. *Cements research progress*. Westerville, OH: American Ceramic Society; 1986. p. 352–79.
- [20] Ginebra MP, Fernandez E, De Maeyer EAP, Verbeeck RMH, Boltong MG, Ginebra J, et al. Setting reaction and hardening of an apatite calcium phosphate cement. *J Dent Res* 1997;76:905–12.
- [21] Ishikawa K, Miyamoto Y, Takechi M, Toh T, Kon M, Nagayama M, et al. Non-decay type fast-setting calcium phosphate cement: hydroxyapatite putty containing an increased amount of sodium alginate. *J Biomed Mater Res* 1997;36:393–9.
- [22] Durucan C, Brown PW. Low temperature formation of calcium-deficient hydroxyapatite-PLA/PLGA composites. *J Biomed Mater Res* 2000;51:717–25.
- [23] Barralet JE, Gaunt T, Wright AJ, Gibson IR, Knowles JC. Effect of porosity reduction by compaction on compressive strength and microstructure of calcium phosphate cement. *J Biomed Mater Res B* 2002;(63):1–9.
- [24] Shindo ML, Costantino PD, Friedman CD, Chow LC. Facial skeletal augmentation using hydroxyapatite cement. *Arch Otolaryngol Head Neck Surg* 1993;119:185–90.
- [25] Friedman CD, Costantino PD, Takagi S, Chow LC. BoneSource hydroxyapatite cement: a novel biomaterial for craniofacial skeletal tissue engineering and reconstruction. *J Biomed Mater Res (Appl Biomater)* 1998;43:428–32.

- [26] Chow LC. Calcium phosphate cements: chemistry, properties, and applications. *Mater Res Symp Proc* 2000;599:27–37.
- [27] Brown GD, Mealey BL, Nummikoski PV, Bifano SL, Waldrop TC. Hydroxyapatite cement implant for regeneration of periodontal osseous defects in humans. *J Periodontol* 1998;69:146–57.
- [28] Shors EC, Holmes RE. Porous hydroxyapatite. In: Hench LL, Wilson J, editors. *An introduction to bioceramics*. New Jersey: World Scientific; 1993. p. 181–98.
- [29] Xu HHK, Quinn JB. Calcium phosphate cement containing resorbable fibers for short-term reinforcement and macroporosity. *Biomaterials* 2002;23:193–202.
- [30] Xu HHK, Quinn JB, Takagi S, Chow LC, Eichmiller FC. Strong and macroporous calcium phosphate cement: effects of porosity and fiber reinforcement on mechanical properties. *J Biomed Mater Res* 2001;57:457–66.
- [31] Takagi S, Chow LC. Formation of macropores in calcium phosphate cement implants. *J Mater Sci: Mater Med* 2001;12:135–9.
- [32] Xu HHK, Simon CG. Self-hardening calcium phosphate composite scaffold for bone tissue engineering. *J Orthop Res* 2004;22:535–43.
- [33] Burguera EF, Xu HHK, Takagi S, Chow LC. High early-strength calcium phosphate bone cement: effects of dicalcium phosphate dehydrate and absorbable fibers. *J Biomed Mater Res A* 2005;75:966–75.
- [34] Burguera EF, Xu HHK, Weir MD. Injectable and rapid-setting calcium phosphate bone cement with dicalcium phosphate dihydrate. *J Biomed Mater Res B* 2006;77:126–34.
- [35] Xu HHK, Eichmiller FC, Giuseppetti AA. Reinforcement of a self-setting calcium phosphate cement with different fibers. *J Biomed Mater Res* 2000;52:107–14.
- [36] Xu HHK, Braum LM, Ostertag CP, Krause RF, Lloyd IK. Failure mode of SiC-fiber-reinforced Si₃N₄ composites at elevated temperatures. *J Am Ceram Soc* 1995;78:388–94.
- [37] Xu HHK, Ostertag CP, Braun LM, Lloyd IK. Effects of fiber volume fraction on mechanical properties of SiC-fiber/Si₃N₄-matrix composites. *J Am Ceram Soc* 1994;77:1897–900.
- [38] Zhang Y, Xu HHK. Effects of synergistic reinforcement and absorbable fiber strength on hydroxyapatite bone cement. *J Biomed Mater Res* 2005;75A:832–40.
- [39] Zhang Y, Xu HHK, Takagi S, Chow LC. In-situ hardening hydroxyapatite-based scaffold for bone repair. *J Mater Sci: Mater Med* 2006;17:437–45.
- [40] International Standards Organization. ISO 10993-5. Biological evaluation of medical devices—Part 5: Tests for in vitro cytotoxicity. International Standards Organization, Geneva, Switzerland, 1999.
- [41] Simon Jr CG, Khatri CA, Wight SA, Wang FW. Preliminary report on the biocompatibility of a moldable, resorbable, composite bone graft consisting of calcium phosphate cement and poly(lactide-co-glycolide) microspheres. *J Orthop Res* 2002;20:473–82.
- [42] Xu HHK, Smith DT, Simon Jr CG. Strong and bioactive composites containing nano-silica-fused whiskers for bone repair. *Biomaterials* 2004;25:4615–26.
- [43] Xu HHK, Simon Jr CG. Fast setting calcium phosphate-chitosan scaffold: mechanical properties and biocompatibility. *Biomaterials* 2005;26:1337–48.
- [44] Boonthekul T, Kong HJ, Mooney DJ. Controlling alginate gel degradation utilizing partial oxidation and bimodal molecular weight distribution. *Biomaterials* 2005;26:2455–65.
- [45] Weir MD, Xu HHK, Simon CG. Strong calcium phosphate cement-chitosan-mesh construct containing cell-encapsulating hydrogel beads for bone tissue engineering. *J Biomed Mater Res A* 2006;77:487–96.
- [46] Lee DD, Tofghi A, Aiolo M, Chakravarthy P, Catalano A, Majahad A, et al. α -BSM: A biomimetic bone substitute and drug delivery vehicle. *Clin Orthop Res* 1999;367S: S396–405.
- [47] Blom EJ, Klein-Nulend J, Wolke JGC, Kurashina K, van Waas MAJ, Burger EH. Transforming growth factor- β 1 incorporation in an β -tricalcium phosphate/dicalcium phosphate dehydrate/tetracalcium phosphate monoxide cement: release characteristics and physicochemical properties. *Biomaterials* 2002;23:1261–8.
- [48] Ruhe PQ, Hedberg EL, Padron NT, Spauwen PHM, Jansen JA, Mikos AG. rhBMP-2 release from injectable poly(DL-lactic-co-glycolic acid)/calcium-phosphate cement composites. *J Bone Joint Surg* 2003;85:75–81.
- [49] Huang YC, Kaigler D, Rice KG, Krebsbach PH, Mooney DJ. Combined angiogenic and osteogenic factor delivery enhances bone marrow stromal cell-driven bone regeneration. *J Bone Miner Res* 2005;20:848–57.
- [50] Isobe M, Yamazaki Y, Mori M, Ishihara K, Nakabayashi N, Amagasa T. The role of recombinant human bone morphogenetic protein-2 in PLGA capsules at an extraskeletal site of the rat. *J Biomed Mater Res* 1999;45:36–41.
- [51] Paralkar VM, Hammonds RG, Reddi AH. Identification and characterization of cellular binding proteins (receptors) for recombinant human bone morphogenetic protein 2B, an initiator of bone differentiation cascade. *Proc Natl Acad Sci USA* 1991;15(88):3397–401.
- [52] R&D Systems. www.RnDSystems.com. Recombinant human BMP-2: Specifications and use. Catalog number: 355-BM, 2005.
- [53] Weir MD, Xu HHK. High-strength, in situ-setting calcium phosphate composite with protein release. *J Biomed Mater Res*, in press.
- [54] Seeherman H, Wozney JM. Delivery of bone morphogenetic proteins for orthopedic tissue regeneration. *Cytokine Growth Factor Rev* 2005;16:329–45.
- [55] Cunningham NS, Paralkar V, Reddi AH. Osteogenin and recombinant bone morphogenetic protein 2B are chemotactic for human monocytes and stimulate transforming growth factor beta 1 mRNA expression. *Proc Natl Acad Sci USA* 1992;89:11740–4.
- [56] Kim HD, Wozney JM, Li RH. Characterization of a calcium phosphate-based matrix for rhBMP-2. *Methods Mol Biol* 2004;238:49–64.